Since January 2020 Elsevier has created a COVID-19 resource centre with free information in English and Mandarin on the novel coronavirus COVID-19. The COVID-19 resource centre is hosted on Elsevier Connect, the company's public news and information website.

Science of the Total Environment 755 (2021) 143050

Contents lists available at ScienceDirect

Science of the Total Environment

journal homepage: www.elsevier.com/locate/scitotenv

Modelling and mapping eye-level greenness visibility exposure using multi-source data at high spatial resolutions

S.M. Labib [a,b,*], Jonny J. Huck [a], Sarah Lindley [a]

[a] Department of Geography, School of Environment, Education and Development (SEED), University of Manchester, Arthur Lewis building (1st Floor), Oxford Road, Manchester M13 9PL, United Kingdom
[b] Centre for Diet and Activity Research (CEDAR), MRC Epidemiology Unit, University of Cambridge, Clifford Allbutt Building, CB2 0AH, Cambridge, United Kingdom

HIGHLIGHTS

- Existing greenness visibility exposure assessment approaches are inadequate.
- We applied viewshed analysis at 5 m intervals for >86 million observer locations.
- The output map provides greenness visibility estimations at any locations in the AOIs.
- Top-down and eye-level greenness visibility are distinct greenness exposure metrics.
- Street-only measures are an incomplete representation of neighbourhood visibility.

GRAPHICAL ABSTRACT

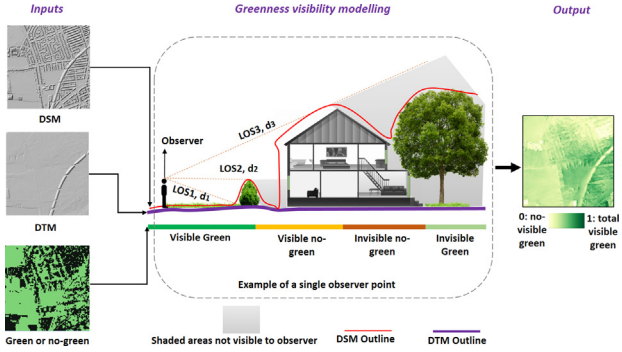

ARTICLE INFO

Article history:
Received 25 July 2020
Received in revised form 8 October 2020
Accepted 8 October 2020
Available online 16 October 2020

Editor: Jay Gan

Keywords:
Greenspace
Eye level greenness visibility
Environmental exposure
Geographic Information Systems
Urban health
Street view

ABSTRACT

The visibility of natural greenness is associated with several health benefits along multiple pathways, including stress recovery and attention restoration mechanisms. However, existing methodologies are inadequate for capturing eye-level greenness visibility exposure at high spatial resolutions for observers located on the ground. As a response, we developed an innovative methodological approach to model and map eye-level greenness visibility exposure for 5 m interval locations within a large study area. We used multi-source spatial data and applied viewshed analysis in conjunction with a distance decay model to compute a novel Viewshed Greenness Visibility Index (VGVI) at more than 86 million observer locations. We compared our eye-level visibility exposure map with traditional top-down greenness exposure metrics such as Normalised Differential Vegetation Index (NDVI) and a Street view based Green View Index (SGVI). Furthermore, we compared greenness visibility at street-only locations with total neighbourhood greenness visibility. We found strong to moderate correlations ($r = 0.65$–0.42, $p < 0.05$) between greenness visibility and mean NDVI, with a decreasing trend in correlation strength at increasing buffer distances from observer locations. Our findings suggest that top-down and eye-level measurements of greenness are two distinct metrics for assessing greenness exposure. Additionally, VGVI showed a strong correlation ($r = 0.481$, $p < 0.01$) with SGVI. Although the new VGVI has good agreement with existing street view based measures, we found that street-only greenness visibility values are not wholly representative of total neighbourhood visibility due to the under-representation of visible greenness in locations such as backyards and community parks. Our new methodology overcomes such underestimations, is easily transferable, and offers a computationally efficient approach to assessing eye-level greenness exposure.

* Corresponding author at: Department of Geography, School of Environment, Education and Development (SEED), University of Manchester, Arthur Lewis building (1st Floor), Oxford Road, Manchester M13 9PL, United Kingdom.
E-mail addresses: sml80@medschl.cam.ac.uk, labib.l.m@gmail.com (S.M. Labib), jonathan.huck@manchester.ac.uk (J.J. Huck), sarah.lindley@manchester.ac.uk (S. Lindley).

https://doi.org/10.1016/j.scitotenv.2020.143050

1. Introduction

The visibility of the natural environment, more specifically exposure to visible greenness, is associated with psychological mechanisms of positive health outcomes, as elucidated by attention restoration theory (Kaplan and Kaplan, 1989; Kaplan, 1995; Kaplan, 2001) and stress recovery theory (Ulrich, 1984; Ulrich et al., 1991; Brown et al., 2013). Nevertheless, analyses of the health benefits of the natural environment tend to rely on measures of blue and greenspace availability and/or accessibility. This reliance has emerged partly due to the relative ease of developing associated exposure metrics based on satellite images (e.g., Normalised Differential Vegetation Index - NDVI) or other spatially explicit data (e.g., land cover) (Zhan et al., 2020; Huang et al., 2020; Browning and Lee, 2017). However, these availability and accessibility metrics usually do not fully capture all of the pathways through which humans experience nature (Labib et al., 2020a; Lindley et al., 2019; Díaz et al., 2018), in part due to such metrics being derived from a top-down 'bird's eye' view in 2D space (x, y) (Labib et al., 2020a; Wang et al., 2020). By contrast, greenness visibility is calculated considering the vertical dimension (Larkin and Hystad, 2019; Jiang et al., 2017), permitting a more representative measure of the human-centric observation of greenness while standing at ground level ('eye-level').

Sight and colour shape our perception of the landscape (Bell, 2012; Russell et al., 2013). While the top-down, bird's eye view, approach to measuring greenspace availability provides an indication of the amount of greenness in a given area (James et al., 2015; Markevych et al., 2017), individual experiences of greenness and awareness of nature also rely on the extent to which green elements of the landscape are visible (Bratman et al., 2019; Silva et al., 2018; Frumkin et al., 2017). Thus, accurately measuring greenness visibility exposure is crucial in understanding how the experience of nature supports the health benefits arising from the natural environment in human surroundings (Li and Ghosh, 2018; Nutsford et al., 2016; Brown et al., 2013). Despite the importance of visibility, it is the least studied exposure metric in current studies exploring the associations between the natural environment and health (Labib et al., 2020a; Dadvand and Nieuwenhuijsen, 2019). It may be speculated that this is due to limitations in existing methodologies for measuring and mapping greenness visibility over large study areas. Omission of explicit greenness visibility metrics may be particularly important in urban environments where there is limited green infrastructure supporting nature's contributions to people (Tzoulas et al., 2007; Díaz et al., 2018; Helbich et al., 2019).

Environmental psychologists use photographs or questionnaires to understand how the visibility of natural features influence attention restoration or stress recovery (Kaplan and Kaplan, 1989; Brown et al., 2013). However, photographs are vulnerable to distortion and provide limited understanding of the visibility of nature in spatial contexts (Anguelov et al., 2010; Furnari et al., 2016). Questionnaires are also vulnerable to subjective responses (Van Herzele and de Vries, 2012; Lottrup et al., 2013; Hazer et al., 2018). These issues, as well as time and resource constraints, frequently prohibit the use of photographs and questionnaires in large cohort-based ecological studies.

More recently, several studies have used street view (SV) images (e.g., Google Street View, Baidu Street View) to objectively measure the visibility of nature, particularly in urban areas (Liu et al., 2020; Helbich et al., 2019). Coupled with artificial intelligence methods (e.g., deep learning), SV-based visibility measurements are becoming increasingly common in the literature (Helbich et al., 2019; Wang et al., 2019, 2020; Ye et al., 2019). However, such approaches have several limitations, chiefly that such SV images are typically only available for streetscapes where there is vehicular access. Thus, relying on SV images results in many locations not being accounted for; including back gardens (Rzotkiewicz et al., 2018; Lu, 2019), the interiors of community parks and public rights of way.

Existing studies using SV images for greenness visibility analysis typically use sample SV images taken along roads within a given neighbourhood and average the sample results in order to determine a visibility value (Lu et al., 2018; Helbich et al., 2019; Lu et al., 2019). Such studies often define neighbourhoods using buffers at various distances (e.g., 400, 800 m) from a fixed location. Alternatively, studies have used administrative boundaries as proxies for neighbourhood definition (Kumakoshi et al., 2020; Larkin and Hystad, 2019). Such arbitrary boundaries subject SV image based exposure assessment to the modifiable areal unit problem (MAUP; Openshaw, 1981) (Lu, 2019). The MAUP can result in under- or over-estimation of exposure measurement variance (Labib et al., 2020b).

Recent studies have applied machine/deep learning models based on convolutional neural networks (CNN) to estimate greenness in SV images (Helbich et al., 2019; Stubbings et al., 2019). A few studies have also used Photoshop-based colour differencing and object-based segmentation methods to extract greenness data (Ye et al., 2020; Li et al., 2015). The accuracy of CNN is often dependent on the quality of the annotated image sets used for training, the learning algorithm and the quality of object segmentation (Zhou et al., 2019; Lecun et al., 2015). Studies using CNN have reported 80–85% accuracy in greenness data extraction (Wang et al., 2020; Stubbings et al., 2019; Helbich et al., 2019). However, there is uncertainty in the estimation of greenness using SV images, which are often collected using wide-angle and fish-eye lenses (see Anguelov et al., 2010), and stitched together using cylindrical or spherical projections. Optical distortion of the output images results in the pixel-size of a given feature being potentially over- or under-represented depending on its position relative to the lens (Hughes et al., 2008; Furnari et al., 2016). Although such optical distortions can be corrected using image projection transformation, their presence in optical data is likely to cause poor SV image detection of objects. Finally, many global cities have incomplete SV image databases and images are often also subject to temporal mismatch issues (Fry et al., 2020; Rzotkiewicz et al., 2018).

Street view-based systems used to capture greenness visibility exposure have become common. However, GIS-based viewshed analysis can also provide objective estimations of greenness visibility. Viewshed analysis is not limited to street-views, having the advantage of eye-level visibility measurement capability at any location in a landscape (Martínez-Graña et al., 2017; Domingo-Santos et al., 2011). Viewshed-based approaches have long been established as the most popular method in the field of Geographic Information Science (GIS) for analysing landscape visibility (Sahraoui et al., 2016; Fisher, 1996). However, a lack of availability of high-resolution spatial data and the computationally intensive nature of viewshed calculations at scale has limited their application (Carver and Washtell, 2012; Qiang et al., 2019). Nonetheless, two recent studies have applied such methods to estimating greenness visibility. Nutsford et al. (2015, 2016) used a viewshed-based index to measure visibility at neighbourhood centroids for viewing distances between 300 and 6000 m and Tabrizian et al. (2020) estimated the viewshed for vegetation at a viewing distance of 1500 m.

Recent studies have adopted viewshed-based visibility analysis to calculate viewsheds ranging from one to several thousand observer locations within given regions (Nutsford et al., 2016; Tabrizian et al., 2020; Chamberlain and Meitner, 2013). However, there are a number of challenges that these studies have revealed in terms of existing viewshed-based methods for modelling greenspace exposure. For instance: the use of low spatial resolution elevation data provides insufficient granularity for modelling greenness visibility (Qiang et al., 2019; Marsh and Schreiber, 2015); and visibility is assumed to be uniform over fixed viewing distances (Tabrizian et al., 2020; Kuo et al., 2018), without consideration of the distance-decay effect. Such discreet distance measurements undermine the visual significance, magnitude, and distance decay effects on visibility (Bishop, 2002), which account for the greater visual significance of closer objects than those at more distant locations in the viewing field (Palmer, 2019; Kumsap et al., 2005).

To address the methodological limitations noted above, we have extended the classic viewshed approach, such that it may be applied to modelling greenness visibility at high spatial resolutions for large spatial extents (e.g., city-region) while accounting for the distance decay effect of visibility. We used multi-source high-resolution land use and land cover (LULC) data, as well as a digital surface model (DSM) and digital terrain model (DTM) processed from Light Detection and Ranging (LiDAR) imagery to create a very fine spatial resolution Viewshed Greenness Visibility Index (VGVI). We mapped VGVI at a 5 m grid cell resolution covering all locations in the case study area (approximately 86 million observer locations), including those where SV images are unavailable (e.g., back gardens, public rights of way, and pocket parks). To our knowledge, such detailed greenness visibility modelling and mapping methods have not been applied in previous greenness exposure studies.

We evaluated the results from our methodology in two ways. We first assess how well our results correspond with a specific urban neighbourhood setting (i.e. how well they represent visibility). We secondly consider what additional information is generated from the results of our method for estimating visibility exposure compared to commonly-used alternative methods (i.e., what the significance of the results might be for wider applications, such as in studies of the links between environment and health). Representativeness is assessed through ground-truthing a case study neighbourhood using a virtual environment. Significance is assessed by comparing results to: a planar surface representation of greenness (via NDVI); and visibility estimates generated from street view images.

2. Methods and materials

2.1. Case study area

We applied the proposed methodological process to the case of the Greater Manchester metropolitan county, situated in the North West of England. This is a post-industrial city-region comprising an area of about 1276 km^2 and a population of 2.8 million people (Dennis et al., 2018, 2020). The city-region has a diverse landscape pattern, including flat plain areas that give way to hills that rise to 500 m in the north and east (Dennis et al., 2018). We selected this case study area both for its diverse landscape pattern and the presence of diverse greenspace elements such as urban parks, farmland, and river corridors. Moreover, the local authority indicates that there is an ongoing need to enhance green infrastructure and biodiversity in support of healthy living (Labib, 2019; GMCA, 2019).

2.2. Data

Our approach was a fusion of both vertical (e.g., elevation surface) and planar datasets to provide a robust estimation of greenness visibility from a human-centric perspective.

2.2.1. Terrain and surface representation

We used 2 m LiDAR-based DSM and DTM data (Defra Data Services Platform, 2020; Environment Agency, 2019a, 2019b), which we resampled to 5 m in order to increase processing speed while still maintaining a high spatial resolution (Supplementary Fig. S1c, d). We selected a LiDAR-based DSM for its proven ability to represent above-ground elements and estimate visibility with high accuracy (Qiang et al., 2019; Van Berkel et al., 2018; Chen et al., 2015). While the DSM provided an accurate representation of ground surface objects, we used the DTM to take account of the ground terrain of the study area since the ground topography influences the viewing angle and aspect of the observer (Brughmans et al., 2018; Nutsford et al., 2015). For the purposes of the present study, we assumed that the observer was always at ground level when visibility is estimated, with an assumed eye-level observer height of 1.7 m.

2.2.2. Land use and land cover

The greenness data used in this study was obtained from Dennis et al.'s (2018) LULC dataset (Supplementary Fig. S1b), which was produced by synthesising multiple greenspace data sets (e.g., Sentinel-2 satellite images, Ordnance Survey green space layer data, tree canopy data). The dataset provides five categories of land cover and within these classifications 35 detailed land use and land cover sub-classifications for the Greater Manchester area. The LULC data demonstrated a satisfactory 85% accuracy level. The LULC data was captured in summer, reflecting summer-time levels of greenness. The present study focused on overall greenness rather than on individual greenspace typologies. Therefore, LULC categories were reclassified into a binary surface of 'green' and 'not green' and resampled to 5 m resolution to keep consistency with the DSM data.

2.2.3. Other data

In order to compare and evaluate our visibility modelling outputs, we considered four additional datasets. The first two were a building dataset and a tree canopy dataset with elevation data, obtained from OS MasterMap Building Height Attribute (OS MasterMap, 2019) and a tree database (City of Trees, 2011) respectively. These two layers were used to visually compare our visibility outputs in a virtual environment. The third dataset was an NDVI layer processed from Sentinel-2A images (10 m) collected on 4th July 2018, with cloud cover <2%. Atmospheric correction of the images was undertaken prior to analysis. We used Sentinel-2 images because they yield higher overall accuracy for detecting vegetation in urban settings compared to relatively low-resolution imagery such as Landsat-8 (Labib and Harris, 2018). Fourth and finally, we also collected Google street view images at sample locations (sampling details in Section 2.5) to compare the output of our visibility model with the street view-based green view index (SGVI).

2.3. Greenness visibility modelling

In this study, we implemented a distance-weighted viewshed algorithm to estimate the visibility of greenness at 5 m intervals (i.e., the cell size of the DTM raster) for the entire study area. Fig. 1 illustrates the overall process. The inputs are DSM, DTM and greenness layers. The modelling process implements multiple line-of-sight (LOS) analyses with a distance decay weighting to identify the visible and obstructed (non-visible) greenness for a given viewing distance in all directions. It then produces a greenness visibility map layer with visibility values ranging between 0 and 1. LOS is the line segment between the point of observation and target points allowing determination of the visibility of target points (Feng et al., 2015; Qiang et al., 2019).

2.3.1. Distance decay model

Generally, the visual prominence of an object in space reduces with increasing distance from the observer (Kumsap et al., 2005; Chen et al., 2015; Taylor and Openshaw, 1975). To take account of this phenomenon and realistically measure the reduction in visual significance of vegetation with increasing distance, we applied a distance decay model to the viewshed analysis. Kumsap et al. (2005) and Bishop (2002) argued that visibility decay could be expressed mathematically as an exponential or power function. Based on several previous studies (Anderson and Rex, 2019; Palmer, 2019; Bishop, 2002), we developed a function to express the distance decay weights. In the decay modelling, we considered several viewing distance bands suggested by Palmer (2019), including; immediate (≤20 m), foreground (400 m), near middleground (2400 m), far middleground (4830 m), near background (8050 m) and far background (16,090 m). For each distance band, we selected a weight value based on values derived from the studies of Anderson and Rex (2019) and Bishop (2002). Both studies empirically estimated the decay weight based on both experimentation and expert opinions. Using these distance bands and corresponding weights, we plotted the

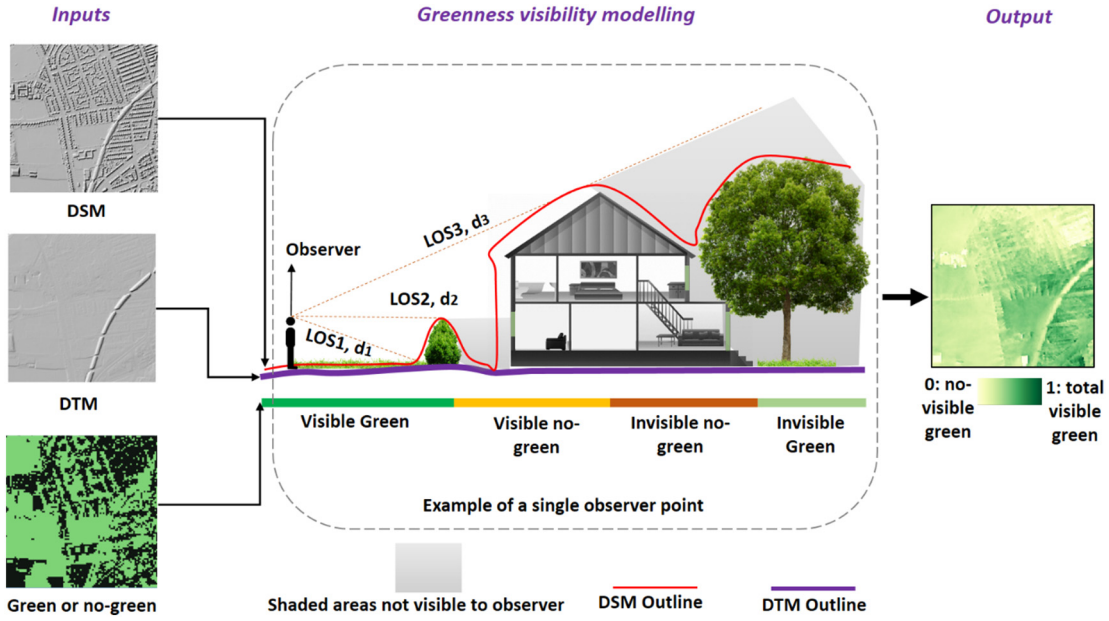

Fig. 1. Conceptual design of greenness visibility modelling. The input layers show the data used in modelling, and the modelling step indicates the process, the output indicates the outcome of the modelling. LOS: line-of-sight, d- distance decay weight. DSM outline in red, DTM outline in purple. (For interpretation of the references to colour in this figure legend, the reader is referred to the web version of this article.)

weights with distance bands and fitted an exponential model ($R^2 > 0.99$) in order to define the relationship (Fig. 2).

The decay function is an expression of how humans actually observe different objects in space and attempts to provide realistic weighting values, using empirical studies to define the reduction in visual prominence of features with increasing distance from the observer. This is important because objects closer to the observer provide more observed detail and clarity (Kumsap et al., 2005; Bishop, 2002) and so have a greater influence on the perception of greenness and positive health outcomes than distant greenspaces (Ulrich, 1984; Ulrich et al., 1991; Nutsford et al., 2016). Nevertheless, the effect is very rarely considered in visibility analyses in an explicit way.

The distance decay model also helps mitigate bias towards further away features that is caused by small increases in viewing distance leading to disproportionate increases in the number of cells falling within the buffer (increase defined by Eq. (1)).

$$n\ cells = \frac{\pi \times radius^2}{resolution^2} \quad (1)$$

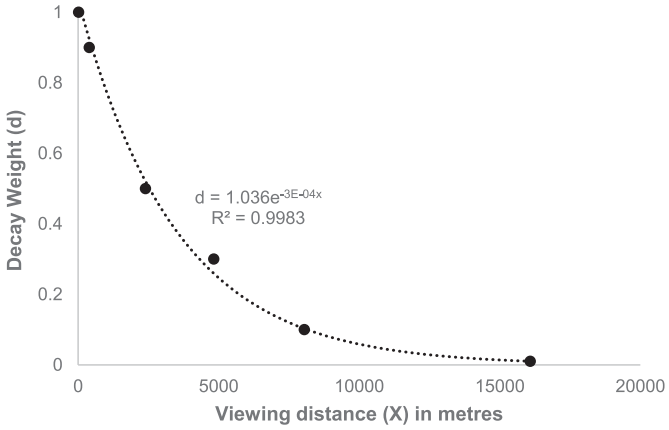

Fig. 2. Distance decay weight function diagram for eye-level visibility.

This effect means that areas distant from the observer are more heavily represented than closer ones because there are a greater number of cells further away than there are close by. In an unweighted measurement (e.g., used in mean NDVI estimation using varying buffer distances), both proximal and distant cells all equally weighted. Therefore, relatively modest increases in buffer distance lead to substantial reductions in the relative importance of the cells in areas immediately surrounding the observer in comparison with those further away. This situation is clearly at odds with human perception, in which closer objects would be expected to be more important. Accounting for visibility (using the viewshed) and observer proximity (using an empirical distance-decay function) permits these problems to be mitigated, and a better representation of reality achieved.

2.3.2. Viewshed algorithm and viewshed greenness visibility index (VGVI)

Traditional viewshed algorithms are often computationally intensive, making them difficult to apply to very large numbers of observer points (Carver and Washtell, 2012). In the present study, modelling visibility was for a high spatial resolution and very large spatial extent, meaning that viewshed calculations for >86 million observer locations were required. In order to achieve this, we developed a lightweight, parallel viewshed algorithm in Python to calculate the greenness visibility index (code details: https://github.com/jonnyhuck/green-visibility-index). Our implementation used the Midpoint Circle Algorithm (derivation details in Cao et al., 2020; Van Aken, 1984) in order to calculate the cells on the perimeter of the viewshed area (Fig. 3a); and Bresenham's line algorithm (Bresenham, 1965, 1977) to determine a LOS from the origin to each perimeter cell, with a fixed observer height of 1.7 m (approximate eye level for an observer located on the ground). Bresenham's algorithm is considered one of the fastest and most efficient methods of formulating line-of-sight calculations (Chung and Huang, 2007; Kappel, 1985).

In the present study, the binary visibility of each cell on the ray was calculated with simple geometry, and accounted for the effects of atmospheric refraction and the curvature of the Earth using standard formulae. The DSM was used to account for obstacles to visibility such as buildings (Fig. 1), whereas relative observer ground elevations were calculated using the DTM. Following Palmer (2019), we applied a maximum viewing distance of 800 m, which corresponded to the

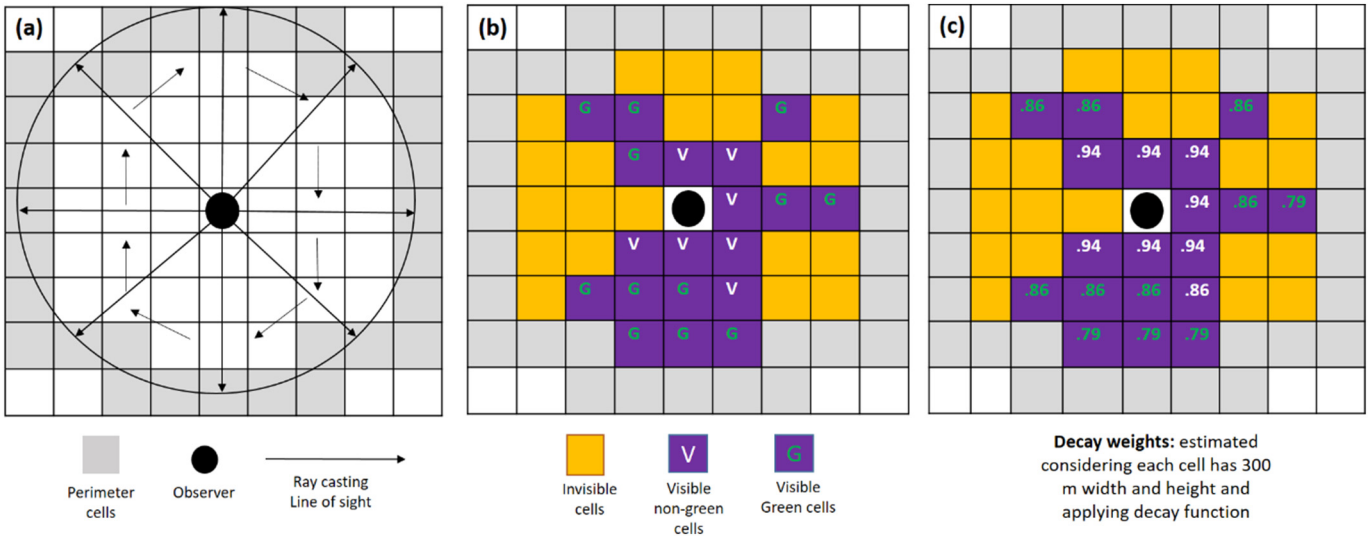

Fig. 3. Example of (a) Line-of-sight algorithm for viewshed analysis for a given viewing distance, (b) viewshed outcome for observer cell; (c) the decay weights associated with the visible cells. For this particular observer cell, VGVI = 0.72; estimated using decay weights in (c) and Eq. (2).

foreground through to the near middle-ground viewing range. This is in line with several recent studies that suggest distances below 800 m as the acceptable range for greenness visibility analysis in urban environments (Helbich et al., 2019; Yang et al., 2019; Lu et al., 2019).

For a given observer location, the algorithm calculated a matrix of binary values representing visible cells, and one for green cells. These were multiplied together to give a matrix of cells that are both visible and green (Fig. 3b), and then with a pre-calculated matrix of weights (Fig. 3c) based upon the decay function calibrated in Section 2.3.1. The algorithm then computed the weighted sum of visible green cells and all visible cells to determine the VGVI for each observer cell using Eq. (2).

$$VGVI_j = \frac{\sum_{1}^{n} G_i \times d_i}{\left(\sum_{1}^{n} G_i \times d_i\right) + \left(\sum_{1}^{n} V_i \times d_i\right)} \quad (2)$$

where, *VGVIj* is the index value for the observer cell *j*; *Gi* is the visible green cell, *Vi* is the visible non-green cell, and *di* is distance decay weight corresponding to visible cell *i*. The estimated VGVI values range between 0 and 1, where 0 = no green cells are visible, and 1 = all of the visible cells are green. Thus, the VGVI value, calculated at 5 m spatial resolution for every cell, expresses the proportion of the total viewshed that comprises greenness for an observer standing on the ground at any given point within the study area.

2.4. Implementation

VGVI estimation was performed at 5 m resolution for the entire study area, resulting in 86,807,875 observer locations. Each observer point required 0.8 s to run the analysis described in Section 2.3.2. Given the computational workload, the analysis was performed using a high-performance computing (HPC) facility at the University of Manchester, running the CentOS operating system and Anaconda Python. Prior to analysis, the study area was divided into 65 equal area subsets using the 'Polygon Divider' plugin for QGIS (https://github.com/jonnyhuck/RFCL-PolygonDivider). Each of the 65 subsets was run as a separate job in a batch array, each of which had access to 16 × 2.60GHz processing cores and 512GB of RAM. Within each batch job, the subset was further subdivided into 16 sub-regions for parallel processing (giving 65 × 16 = 1040 processes in total). The resulting surfaces for each set of 16 sub-regions were stitched and written to temporary files, which were finally stitched together into a single output surface once all 65 subsets had been completed. The whole analysis took approximately 11.5 days, with a total 'clock time' of 1068:54:46 h.

2.5. Evaluations of viewshed greenness visibility index

We evaluated our greenness visibility metric by conducting an exploratory analysis and by comparing the metric with other greenness exposure measurements. The VGVI measure was explored visually by creating a virtual representation of a study neighbourhood using OS MasterMap Building Height Attribute (OS MasterMap, 2019) and a tree database (City of Trees, 2011). This process, with building and tree data overlaid on the VGVI surface allowed investigation of how the presence of obstacles (e.g., buildings) influences greenness visibility. This examination of the data in a virtual environment provided a simple form of visual validation for our modelled greenness visibility.

2.5.1. Comparisons with other greenness exposure metrics

To compare the resulting VGVI surface against other greenness measures that are common in the literature, we have calculated a greenness exposure metric at one hundred random sample locations for comparison. This measure was based on the mean NDVI value (Section 2.2.3) within a 100, 300 and 500 m radius of the observer location. Distance decay was not applied to these data in order to reflect the dominant approach in the literature (Browning and Lee, 2017; Labib et al., 2020a), so as to provide a methodological comparison between that presented here, and common approaches in the literature. These mean NDVI values were compared with the corresponding VGVI values for the 100 sample points using Pearson's correlation coefficient to examine the extent of agreement between the two measures.

VGVI values were also compared with eye-level street view-based SGVI values at 100 random sample points. In this analysis, the SGVI value for each sample location was estimated as the ratio of the number of green pixels per image to the total number of pixels per image summed over the four cardinal directions (details in Chen et al., 2019; and Li et al., 2015). It should be noted that the distance decay has not been explicitly accounted for in SGVI calculations because it is already implicitly accounted for (in that the relative number of pixels representing an object is a function of its distance from the camera). We used the magic wand tool in Adobe Photoshop (version CS6) to extract the green pixel counts from trees, shrubs, and any other vegetation and manually deselected any non-vegetation features (e.g., green paint) following the method applied by Yang et al. (2009). Photoshop-based

manual selection of greenness usually yields greater accuracy for greenness values than automated greenness extraction methods such as machine learning models or object-based analysis. For this reason, previous studies have often used the Photoshop-based manual selection method to validate the automatic greenness extraction methods upon which their studies were based (Yang et al., 2019; Lu et al., 2019). Pearson's correlation coefficient was used to assess the degree of agreement between the VGVI and SGVI values. Cross-correlation tests were also conducted between SGVI and mean NDVI values to explore the consistency of correlation among eye-level and top-down greenness measurements.

2.5.2. Entire neighbourhood and street-only greenness visibility exposure comparisons

We compared VGVI values observed from the street with VGVI values from the surrounding neighbourhoods to understand how far street-level greenness visibility adequately reflects neighbourhood-scale visibility. We selected 15 neighbourhoods in the study area for the comparisons. We followed a quota sampling method (Acharya et al., 2013) to select these neighbourhoods at locations exhibiting a variety of urban morphologies (e.g., dense urban, peri-urban etc.) and with different built environment characteristics (e.g., grid-iron or geometric street layouts). Fifteen Lower Super Output Areas (LSOA) were selected as neighbourhood boundaries (as is common practice in England; Mitchell and Popham, 2008; Office for National Statistics, 2011). For each neighbourhood, a zonal statistics tool (ESRI ArcGIS Pro 2.5) was used to extract mean VGVI values for all cells within the boundary, as well as mean VGVI values for cells on the street network only. A third dataset for comparison comprised mean SGVI values calculated using the method described in Section 2.5.1, using street view images extracted at 50–100 m intervals (depending on LSOA size). Similar methods for deriving values of neighbourhood level greenness visibility for street view images have been applied in several previous studies (Li and Ghosh, 2018, Chen et al., 2019; Lu, 2019; Chen et al., 2020). Across the fifteen selected neighbourhoods, we obtained an average of 22 SGVI values, the mean of which was assigned as the greenness visibility value for the corresponding neighbourhood. Pearson's correlation tests were run in order to examine the relationship between mean neighbourhood VGVI, mean street network VGVI, and mean SGVI.

3. Results

3.1. Distribution of viewshed greenness visibility index

Fig. 4a shows the greenness visibility surface mapped applying the VGVI analysis method developed in the present study. The mean value of the VGVI raster is 0.59, with a standard deviation of 0.27 (Supplementary Fig. S2). These values indicate moderate to high ground-level greenness visibility (~59%) is present in Greater Manchester. However, the spatial distribution of greenness has distinct patterns (Fig. 4a). The highest greenness visibility values are often found at the eastern and north-eastern edge of the study area, along the Pennine Hills (Fig. 4b). Not surprisingly, these areas have high greenness visibility, as these contain wide open natural green areas surrounded by elevated topography and without major constructions (e.g., high-rise buildings) obstructing views (Fig. 4c). In addition, there were several green corridors (usually river corridors), where we observed very high VGVI values. In contrast to the high greenness visibility values, we found very low to moderate greenness visibility within the urban core areas of Greater Manchester (Fig. 4a, b). This was caused by the presence of high-rise buildings, low amounts of urban greenspaces, fragmented areas of vegetation, and flat topography. As might be expected, when comparing Fig. 4a and c, VGVI shows a similar distribution to the binary greenness map. However, closer examination (Fig. 4d, e) reveals that in many locations VGVI values are lower than expected, due to the presence of features such as buildings.

3.2. Evaluations of viewshed greenness visibility index

A virtual exploration of the mapped VGVI values for a case study area is presented in Fig. 5. The case study neighbourhood was selected due to its diversity of VGVI values and spatial distribution of greenspaces and buildings. For this case study area, the VGVI values highlight the influence of the built environment on greenness visibility. For example, Fig. 5(a) depicts considerable open green areas to the left side of the observer with non-obstructed views, resulting in a high VGVI value for location (a). In contrast, at location (b), the visibility of greenness is blocked by the presence of buildings in the surrounding areas, despite the close proximity of greenspace (<100 m). In both cases, when compared with ground-truth images, the modelled VGVI values were a good fit to what an observer could see from these viewpoints. This exploration demonstrates the importance of the built environment layout and organisation of buildings in analysis of greenness exposure, as well as the value of the VGVI for capturing greenness visibility at eye-level.

3.2.1. Comparison of VGVI with remotely-sensed NDVI and SGVI

The correlation between the eye-level greenness visibility for ground observers (i.e., VGVI and SGVI) metrics and the remotely-sensed greenness metric (i.e., NDVI) at different buffer distances is presented in Table 1. We observed significant strong to moderate positive correlations between NDVI and eye-level greenness, with the correlation coefficients decreasing with increasing buffer distance (Table 1). This is a critical observation that demonstrates the importance of both visibility and the distance-decay function, as noted in Section 2.3.1. In the VGVI calculation, the most distant cells have the lowest weights and are most likely to be obscured by intervening features, meaning that they are not visible. Neither of these effects is reflected in the NDVI calculation, which explains the greater mismatches at larger buffer distances between the two measurements.

It was notable that SGVI correlations with NDVI were weaker than VGVI correlations at all three buffer distances (Table 1). This result is likely because LULC data was used in the VGVI estimation, and this metric would likely have stronger correlations with NDVI as both LULC and NDVI were obtained from satellite images. Another reason might be related to the fish-eye effect in SV imagery, whereby greater optical distortions occur for objects further away in the street view images (Hughes et al., 2008; Furnari et al., 2016). It might also be attributed to a lack of imaging clarity in objects beyond a certain threshold distance in street view images (Chen et al., 2020). This sensitivity was characteristic of the methodological difference between VGVI and SGVI measurements. Finally, the results suggest that measures using SGVI may lack completeness due to the restricted locations at which SV images are taken.

When the VGVI and SGVI values were compared, we found a significant positive correlation ($r = 0.481$, $p = 4.01 \times 10^{-7}$) between these two measurements of eye-level greenness visibility (Fig. 6). The correlation coefficient implies that in most cases, both methods possessed similar traits in measuring greenness at eye-level. We observed that VGVI values were higher than the corresponding SVGI values in 87% of locations, likely due to generalisation in the input data for VGVI and the underrepresentation of more distant vegetation in SVGI (Chen et al., 2020; Anguelov et al., 2010; Furnari et al., 2016). Chen et al. (2020), for example, noted that Baidu street view images could identify objects clearly to a distance of 220 m, beyond which green objects might not be clearly detected. It should also be noted that most SGVI calculations (including those implemented here) do not mask the sky from the image, which may result in systematic underrepresentation of eye-level greenness. Nevertheless, while there are methodological differences between viewshed and street view-based estimations of greenness visibility, both methods generate similar patterns in eye-level greenness visibility measurement and modelling.

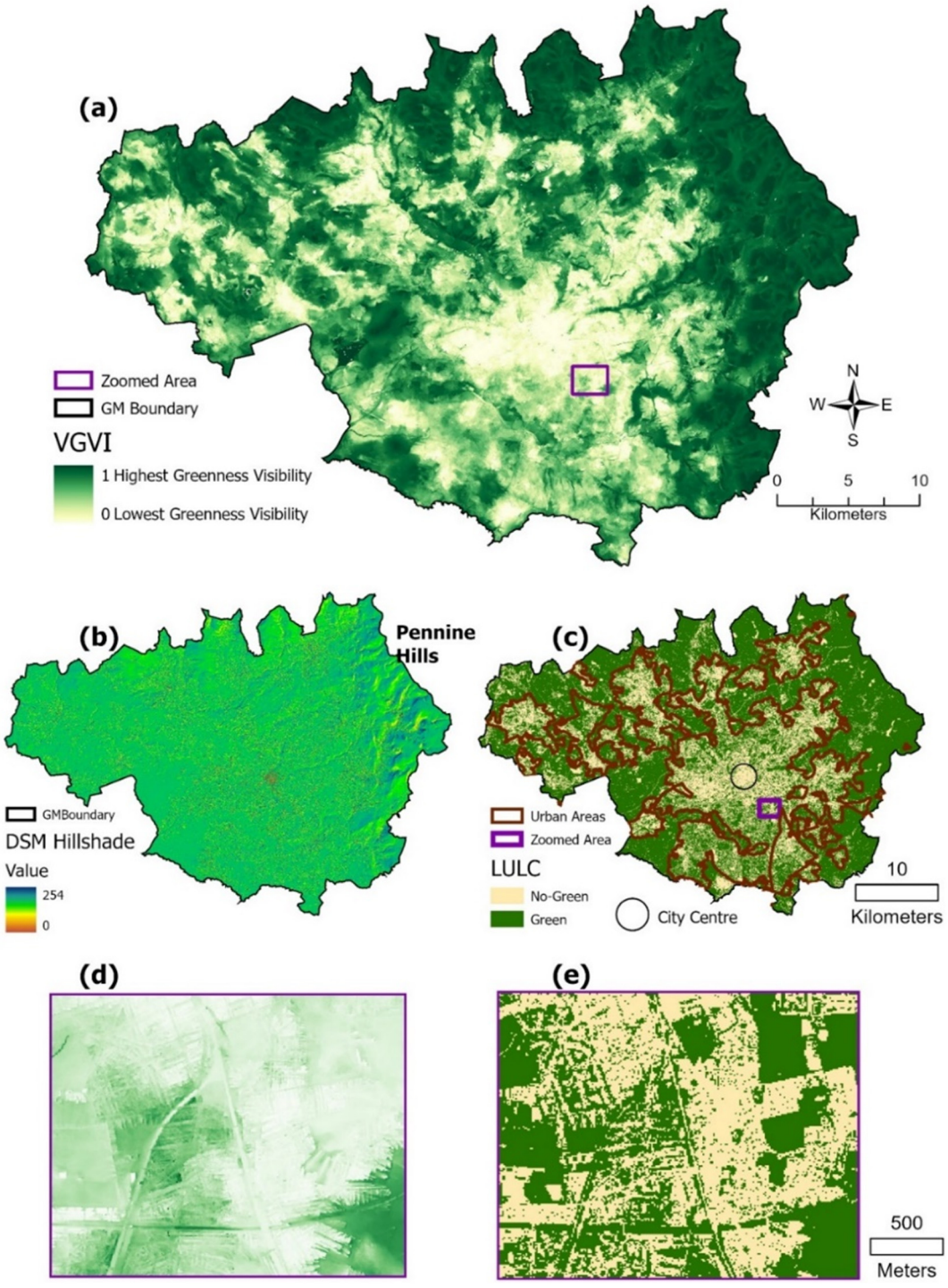

Fig. 4. (a) Viewshed greenness visibility index map, (b) DSM map patched with DTM values for Pennine Hills indicating height (m) distribution, and (c) binary green, no-green map with urban area boundaries, (d) extended case study area of greenness visibility, (e) extended cases study area of binary green, not-green map. (For interpretation of the references to colour in this figure legend, the reader is referred to the web version of this article.)

3.2.2. Comparisons of neighbourhood scale mean greenness visibility measurements

The correlation analysis between different greenness visibility measurements at the neighbourhood scale are presented in Supplementary Table S1. We observed a very strong significant positive correlation ($r = 0.93, p < 0.01$) between neighbourhood mean VGVI values (including all VGVI cells within a given neighbourhood boundary) and mean street-only VGVI values (including VGVI cells on streets) for all 15 sampled neighbourhoods. This result implies that greener neighbourhoods usually have higher greenness visibility on streets. However, when the mean greenness visibility values of the neighbourhood and street-only values were compared, we found significant differences between the two ($t = 2.265, p = 0.04$, details in Supplementary Table S2), with an absolute maximum difference value of 0.17 (~17%), and a mean of 0.05 (~5%). This result indicates that the mean greenness values on street-only locations can be significantly different from the total neighbourhood mean visibility, although they show similar greenness visibility patterns. In addition, the correlation between total neighbourhood mean VGVI values and mean street view (SGVI) values for the corresponding neighbourhoods was positive but insignificant

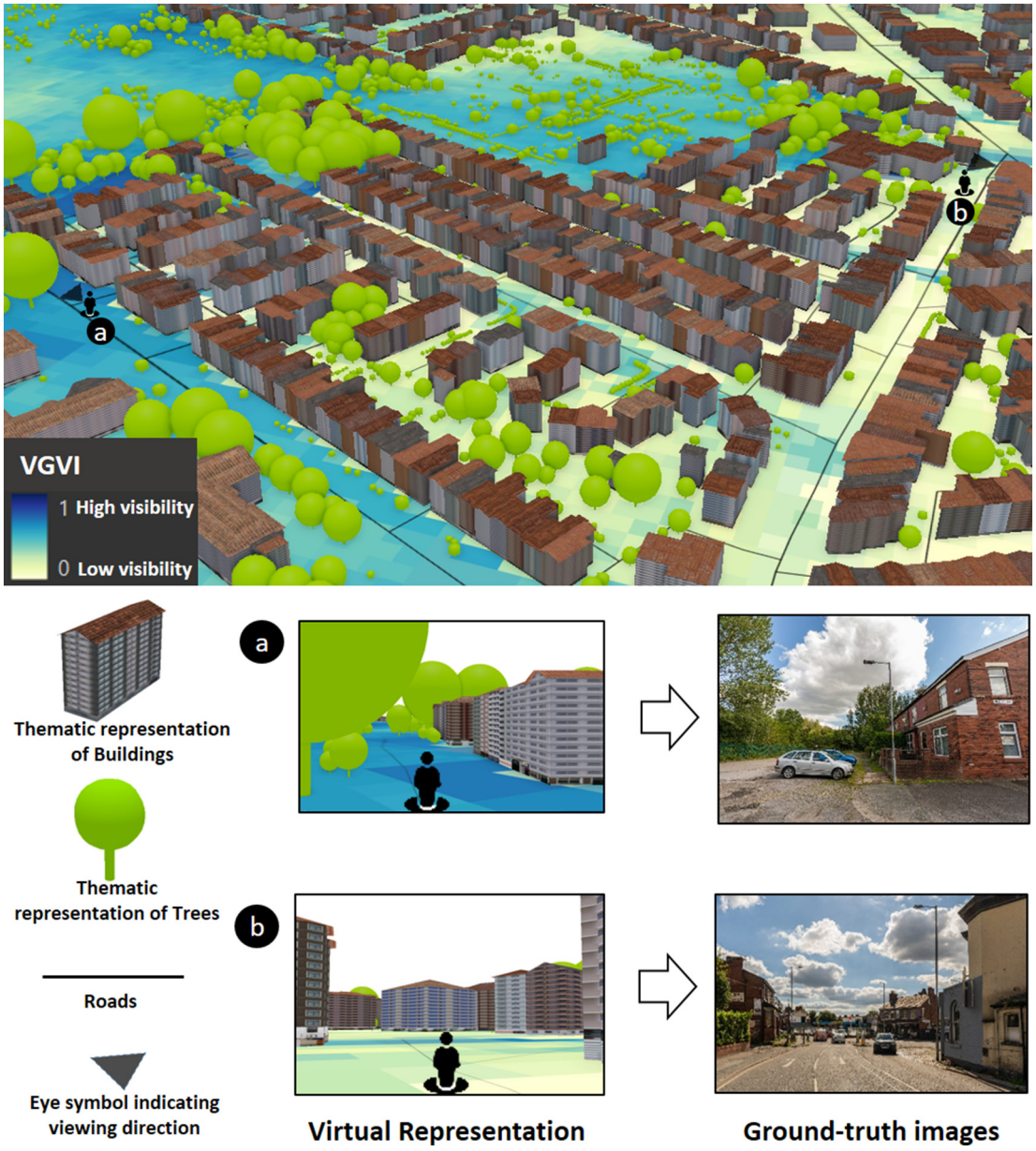

Fig. 5. Virtual representation of buildings and trees on the VGVI map and comparing with ground-truth images for location (a) and (b). Ground-truth photos taken by the lead author. Short virtual tour available at: https://youtu.be/71xdj7hv2HE.

($r = 0.434$, $p = 0.106$, Supplementary Table S1). This result indicates that total neighbourhood greenness visibility might not always reflect the greenness observed from street-only locations. Interestingly, we observed a strong positive correlation ($r = 0.572$, $p = 0.026$, Supplementary Table S1) between street-only mean greenness values for neighbourhoods for both VGVI and SGVI methods. This result confirmed that when street-only means are considered, both VGVI and SGVI can indicate similar patterns of greenness visibility for neighbourhoods.

Table 1
Pearson's correlation coefficients between eye-level greenness visibility and top-down greenness metric at different buffer distances.

Top-down values (mean)	VGVI	SGVI
NDVI (100 m)	0.653	0.56
NDVI (300 m)	0.623	0.514
NDVI (500 m)	0.50	0.426
N	100	100

All correlations are significant at the 0.01 level (2-tailed).

4. Discussion

4.1. Greenness visibility exposure modelling and mapping

In this study, we introduced a quantitative approach to assess the visibility of greenness at eye-level (1.7 m) by combining high-resolution spatial data from multiple sources. We applied this new method to the case study area of Greater Manchester in order to model and map greenness visibility for >86 million observation locations (covering an area of approx. 1276 km^2). Our method combined efficient algorithm design and parallel computing to permit the analysis of many more observation points than has been achieved in other recent studies, which typically utilise from a few hundred to several thousand observation points (e.g., Nutsford et al., 2016; Chen et al., 2020; Tabrizian et al., 2020; Lu, 2019). Our exposure modelling and mapping approach provides a viable methodological solution for large-scale socio-ecological studies investigating the associations between greenness exposure and health outcomes. Methodological efficiency is crucial

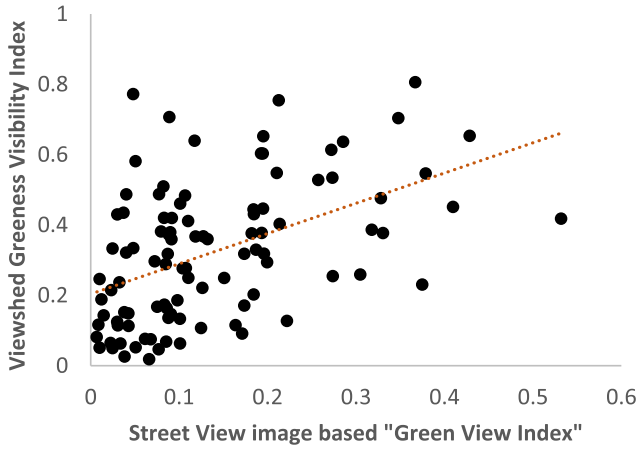

Fig. 6. Correlation ($r = 0.481$, $p < 0.01$) between VGVI and SGVI for 100 locations.

to support the use of more accurate metrics in future epidemiological studies. The majority of existing studies have relied upon top-down 'bird's eye' view remotely-sensed greenness metrics on planar surfaces (mostly NDVI) as opposed to eye-level greenness visibility calculated considering the vertical dimension (Larkin and Hystad, 2019; Jiang et al., 2017). This is due to lack of data resource intensity (e.g., conducting large scale questionnaire-based surveys) and the complexity of modelling approaches to assess greenness visibility at scale (Labib et al., 2020a; Larkin and Hystad, 2019). Our method utilises readily available spatial data that ensure the transferability of this method to other study areas. Thus, a key contribution of this study is to develop and demonstrate a fast, straightforward, and reliable eye-level greenness visibility exposure modelling and mapping methodology allowing utilisation of high-resolution data for an entire city-region.

In addition, our greenness visibility city-region map (Fig. 4a) illustrates the spatial patterns of greenness visibility in the case study area. The map presents an intuitive representation of eye-level greenness visibility, with the lowest VGVI values within high-density urban core areas and the highest values around large natural greenspaces (e.g., near to hills, along riparian corridors). Our findings are consistent with previous studies that indicated built, and natural environment contexts are key to assess eye-level greenness visibility (Yang et al., 2009; Stubbings et al., 2019; Yu et al., 2019).

4.2. Top-down and eye-level greenness exposure

Several previous studies pointed out that top-down and eye-level visibility exposure might not be the same (Chen et al., 2020; Yu et al., 2019; Ye et al., 2019; Li et al., 2015). However, these studies only considered street view image-based visibility measurements for comparison. We have investigated the associations between top-down greenness and eye-level greenness exposure for both viewshed and street view approaches (i.e., VGVI and SGVI). For both metrics, we observed significant differences between top-down and eye-level greenness exposure estimates. In particular, we observed a decrease in the strength of the correlation coefficients with an increase in buffer distance (Table 1). Yu et al. (2019), Ye et al. (2019) and Li et al. (2015) also document a similar trend. The significant strong, positive correlation between top-down and eye-level exposure at smaller buffer distances is reasonable, as greenness (e.g., trees) or objects within proximity are more likely to be clearly visible to an observer.

Nearby objects are less vulnerable to the decay effect than farther objects (Kumsap et al., 2005; Bishop, 2002) and have greater likelihood of being observed. Additionally, in street view images, objects located further away often possess disproportionately low pixel counts due to lens distortion, compared to objects closer to the camera (Anguelov et al., 2010; Furnari et al., 2016). Both the decay effect and lower pixel counts are likely to influence eye-level visibility measurements, but neither is typically accounted for in NDVI-based exposure measurements. Therefore, at larger buffer distances, we observed greater mismatches between top-down and eye-level greenness exposure values. It should be noted that, unlike eye-level visibility, there is no existing empirical research that has investigated the distance decay effect on NDVI values at varying buffer sizes. Thus we could not eliminate the potential that the mismatch between eye-level greenness visibility and top-down greenness measurement with increasing buffer distances may also have stemmed from distance decay effects on NDVI.

Our analytical approach provides a quantification of the differences between eye-level and top-down exposure assessment, and also suggests some possible reasons for the differences that we have found. Based upon these differences, we argue that eye-level greenness visibility is distinct from other greenness metrics that have been developed for greenness exposure assessment and is complementary (but different) to top-down measurement (also Kumakoshi et al., 2020). This is due to the fact that it can capture the vertical dimensions of greenness that relate to human perception and infer the experience of observing the surrounding environment.

4.3. Neighbourhood greenness visibility exposure

Existing studies of the influence of greenness visibility exposure on health usually measure greenness visibility for sampled locations only on streets and use the mean of these values to infer neighbourhood greenness visibility (Li and Ghosh, 2018; Wang et al., 2019, 2020; Lu, 2019). This is because the images that are easily available for use in such analyses are mostly collected on streets. We argue the need for methods that are able to account for measuring greenness at every location within a neighbourhood. This is particularly important in landscapes with complex land cover compositions and where there are lower road densities (including rural areas, which generally the exhibit the highest visibility values in our analysis). This argument is supported by Mavoa et al. (2019), who noted that the health benefit of the visibility of nearby greenery does not operate only along road networks.

Despite having a positive relationship, we found that measurements of street-level greenness visibility provided significantly different values to those provided by our methodology (see Section 3.2.2 and Supplementary Table S2). Additionally, the correlation between the neighbourhood average street view green view index (SGVI) and VGVI was insignificant ($r = 0.434$, $p = 0.106$, Supplementary Table S1). This evidence suggests that the traditional approach of inferring street only visibility as functionally equivalent to neighbourhood greenness visibility needs careful consideration. Our analysis suggests that mean street-based greenness visibility can significantly differ from entire neighbourhood scale greenness visibility, even where they illustrate similar trends in visibility.

We have identified two key reasons for such differences. Firstly, street-only visibility clearly cannot take account of greenness visibility in locations where streets are not available (e.g., backyards or community gardens). This causes an underrepresentation of visible greenness. Secondly, neighbourhood morphology (e.g., street layout) can determine how much greenness is visible from the street. In particular, grid-iron street layouts with densely arranged terraced houses often demonstrate low greenness visibility from the street (Supplementary Fig. S4a, b). Characteristically, these streets contain fewer street trees and exhibit 'street canyon' morphologies (streets bounded by buildings on both sides with few gaps, Fig. 5, location-b) which can obstruct visibility significantly. However, the presence of backyard gardens and pocket parks sometimes account for higher greenness visibility values than street-only visibility values would suggest (Supplementary Fig. S4a). In contrast, neighbourhoods with more curvilinear or looped street layouts and greater inter-building gaps usually show more similar greenness visibility both for the street-only and overall neighbourhood averages (Supplementary Fig. S4 c, d). Additionally, although street-

only visibility is lower than the total neighbourhood visibility for the majority of the neighbourhoods, in a few cases we found the street-only greenness visibility can be higher than the neighbourhood greenness visibility. In these cases, the neighbourhoods possess streets that are located beside large open greenspaces, have a mixed street layout (e.g., curvilinear, cul-de-sac, and grid), and may also co-exist with dense street tree cover (Supplementary Fig. S4e, f). We also found that densely built neighbourhoods had a significant negative correlation with both street-only and overall neighbourhood greenness visibility (see Supplementary Table S3). These issues further show why greenness visibility measurements require a more critical approach. Street-only measurements generally underestimate or, in special cases, overestimate the greenness visibility depending on the neighbourhood morphology.

Measuring greenness visibility exposure as a continuous surface permits a deeper understanding of visibility exposure at non-street locations, such as in a garden or local park. This greenness visibility may have a considerable effect on health outcomes (de Bell et al., 2020; Clayton, 2007). Several studies have found that spending time in a backyard or in community gardens is associated with positive health benefits (e.g., restoration of attention, stress reduction) and just viewing greenness while relaxing in a garden positively influences wellbeing and happiness (Church, 2018; Freeman et al., 2012; Clayton, 2007; Kaplan, 2001). Such greenness visibility can be expected to have had positive health benefits during the 'lockdown' periods associated with the COVID-19 pandemic, for example (Daniela et al., 2020). In order to better assess these benefits, it is important to go beyond an assessment of the availability of garden space (Brindley et al., 2018) and account for the visibility of green cover, impacts from nearby spaces, and the context of wider landscapes. We therefore argue that greenness visibility exposure assessment should reach beyond the streetscape and consider all locations in an entire neighbourhood. The method that we developed for this study can provide such detailed measurements of greenness visibility exposure.

4.4. Implications of eye-level greenness visibility exposure mapping

Our metric and associated transferable methodology have several practical and policy implications. For socio-ecological and epidemiological studies investigating associations between nature and human health, our greenness visibility exposure modelling and mapping can be used as a new metric to evaluate the visual impact of greenness on health. It improves upon existing greenness exposure assessment methods by taking account of vertical dimensions, providing measurements at a high spatial resolution and over large spatial extents. Our approach minimises several limitations of other methodologies, including measuring greenness visibility in locations where street view images are unavailable, modelling visibility at a limited number of sample locations, relying on sophisticated resource-intensive modelling techniques (e.g., deep learning) and privacy issues associated with using street view images. Additionally, the greenness visibility map can estimate dynamic (e.g., spatiotemporal variation) greenness visibility exposure to understand the variance of visibility at different locations beyond the neighbourhood (Helbich, 2018). Such an application is illustrated in Fig. 7, in which an observer has a VGVI value of 0.43 at home (moderate visibility), 0.07 at the office (very low visibility), and varying greenness visibility along the roads to which they are exposed in daily travel. With additional data such as GPS tracks, spatial diary data, our greenness visibility exposure map can provide a comprehensive measurement of daily exposure to greenness at eye-level.

Our new greenness visibility modelling and mapping approach has applications in urban planning and design. In practice, planners and designers could use the map to allocate resources in areas where greening interventions are most needed in terms of improving eye-level greenness. This would allow better optimisation of the limited available resources to maximise greenness visibility. Notably, our approach would allow planners and designers to identify strategic locations and future street layouts, as well as their sizes and types of greenspaces to ensure the greatest possible greenness visibility for such locations in order to

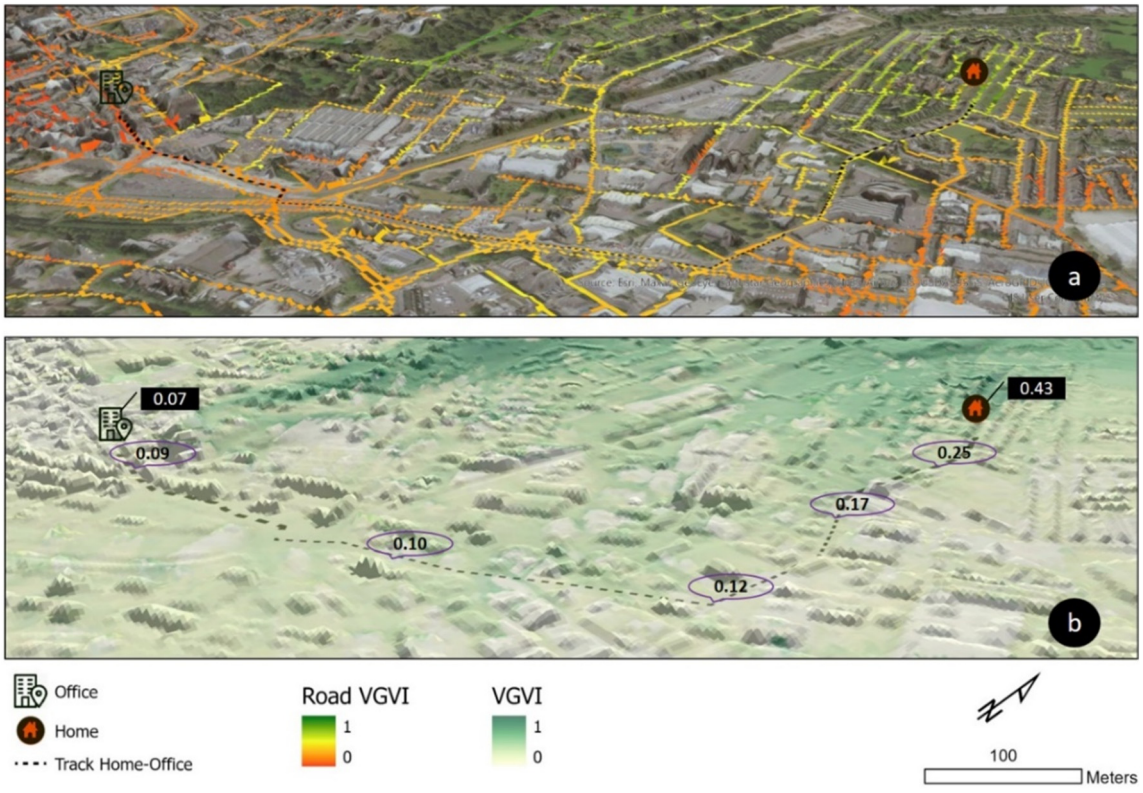

Fig. 7. (a) Road greenness visibility overlaid on a high resolution satellite image and elevation layer, (b) difference in greenness visibility (VGVI) exposure at varying locations (e.g., home, office, along roads).

maximise broader public health benefits. This approach can also be used to evaluate the before and after changes of new planting initiatives in the city; this would inform local councils on the real-world impact of tree planting schemes as well as the removal of vegetation.

In addition to research and practice usage, our greenness visibility exposure maps could also be useful to the general public. We developed an online web map portal to disseminate our results to a broader population (https://arcg.is/1vumGC0). The road VGVI map can be useful for home-owners associations seeking to improve their neighbourhoods as well as people who wish to evaluate and select greener routes for their daily travel. Also, with a simple postcode search people can quickly identify the level of greenness visibility surrounding their home.

4.5. Limitations and future developments

Despite its potential, the method presented in this paper has a number of limitations and there is scope for enhancing it based on potential future developments. The reliability of the modelling depends on the spatial resolution of input data (e.g., DSM, LULC). We modelled and mapped greenness visibility at 5 m spatial resolution; however, it is possible that our LULC map has misclassified small greenspaces sized less than 25 m^2, and that the DSM has underestimated the height of smaller objects. Similarly, smaller objects, such as power lines and street lights, will have been excluded from the analysis through generalisation, meaning that their impact will not be included in the analysis. These issues could to some extent be resolved to an extent by using even higher spatial resolution data (e.g., DSM <1 m resolution), though there would be a proportionate increase in calculation runtime. Our input data also does not take account of vertical vegetation cover such as green walls. However, this limitation is acceptable as such sources of greenness represent a very small portion of overall greenness observed in urban areas (Dennis et al., 2020).

In the present study, due to the computational budget required to process >86 million observer locations, we selected for a viewing distance of 800 m. This might have underestimated the visibility for greenness located beyond this viewing range. Based on our experimental observation in the case study area, we argue that for urban areas with similar characteristics to our study area 800 m appears a reasonable distance for visibility analysis (Helbich et al., 2019; Lu et al., 2019), however sensitivity analysis at longer viewing distances is needed to identify if there are other more appropriate viewing distance for greenness. For future studies, the effect of larger viewing distances should also be tested. However, care should be taken with longer viewing distances, as such distances are often affected by prevailing meteorological and air quality conditions (e.g., lack of clarity due to haze) in real-world settings, which might need to be considered in the model.

In our visibility model, we assumed our observer always stood on the ground, which will result in some under estimation of greenness visibility for residents of multi-story buildings. Although varying observer heights can be integrated into our algorithm, such integration would need to be done with care, as in multi-story buildings the observer location will differ depending not only on what floor the observer is on but also on the height, position of windows or openings in the building (Yu et al., 2016).

One key aspect of this study is that we modelled and mapped greenness by combining different vegetation types (e.g., trees, grass) for overall greenness visibility. Such a combined approach has some benefits such as providing a holistic estimation of all visible green elements. However, this combined approach might also have generalised the potentially differing influences of different vegetation types as argued by Wang et al. (2020) and Kaplan and Kaplan (1989). Because different vegetation types usually have varying qualities (e.g., the visual quality of large tree patch is different to a grass patch) the differing qualities of greenness might also influence the impact on overall health. However, it should be noted that our methodology is fully capable of measuring greenness visibility for different greenness types. For example, we can map only the visibility of trees by using a binary layer indicating the presence/absence of trees. Such detailed visibility mapping of different vegetation types should be explored in further studies. Additionally, vegetation with different colours and covers in different seasons need to be explored.

In this study, the decay model we applied in visibility analyses was constructed based upon previous empirical studies in different contextual setups than our case study area. However, further work is required in order to understand how sensitive this method is to variations in the parameters of the decay function. Though a sensitivity analysis such as this is beyond the scope of this paper, a detailed sensitivity analysis of the decay function in relation to different geographic and landscape locations would be beneficial in future research.

We evaluated our computationally-modelled greenness visibility outputs in a virtual environment, which allowed us to compare results with images captured in the study area. Visual validation of the results indicates that the modelled greenness visibility matches with expectations from both virtual and ground observations (Fig. 5; Supplementary Fig. S3). However, detailed empirical validation comprising large-scale ground truthing and matching with human perceptions would be a valuable addition. Future research in this area might include validation using human perception (Brown et al., 2013) and immersive virtual environment surveys (Tabrizian et al., 2020; Browning et al., 2019).

Finally, we only considered greenness visibility in this particular study but several studies have suggested that the visibility of blue spaces can also have a considerable health impact (McDougall et al., 2020; Nutsford et al., 2016). Once again, our method can easily be adapted to account for blue space visibility. In future studies, a combined green and blue space visibility exposure assessment approach should be developed to understand the overall visual impact of nature on health and wellbeing.

5. Conclusion

In this study, we present an innovative methodological solution to the assessment of greenness visibility exposure at high spatial resolutions using multi-source spatial data, viewshed modelling and distance decay weighting. We demonstrate how top-down and eye-level greenness measurements differ for a large city-region in northern England. Our greenness visibility results show strong to moderate correlations ($r = 0.65–0.42$, $p < 0.05$) with mean NDVI as a commonly-used measure of greenness exposure. However, the decreasing trend in correlation strength at increasing buffer distances from observer locations indicates how NDVI alone is a limited proxy for assessing greenness exposure. Similarly, despite our results showing good overall agreement with street view-based measures ($r = 0.481$, $p < 0.01$), the latter can lead to serious underestimation of neighbourhood-scale visibility.

Our methodological approach overcomes many problems with existing greenness visibility exposure assessment methods identified in the literature, and has the benefit of being easily transferable to any areas where existing land cover and digital elevation model data are available. Furthermore, this methodology also has relevance and significance beyond the study of greenness exposure assessment. For example it can be used in other environmental 'landscapes' associated with visibility modelling, such as in the assessment of aesthetic potential in landscape management.

CRediT authorship contribution statement

S.M. Labib: Conceptualization, Methodology, Data curation, Formal analysis, Investigation, Software, Writing - original draft, Visualization. **Jonny J. Huck:** Supervision, Methodology, Software, Resources, Writing - review & editing. **Sarah Lindley:** Supervision, Resources, Methodology, Writing - review & editing.

Declaration of competing interest

The authors declare that they have no known competing financial interests or personal relationships that could have appeared to influence the work reported in this paper.

Acknowledgments

We would like to thank the reviewers and editor of this paper for their constructive comments and suggestions. We acknowledge the use of Environment Agency data, © Environment Agency copyright and/or database right 2015. We also acknowledge the use of OS MasterMap Building Height Attribute dataset under Educational User Licence and © Crown copyright 2019. Our VGVI software relies upon the Fiona, Rasterio, Numpy, Shapely and SkImage Python libraries. We would also like to acknowledge the assistance given by Research IT and the use of the Computational Shared Facility at The University of Manchester. S.M. Labib is funded by the School of Environment, Education and Development Postgraduate Research Scholarship at the University of Manchester. Elements of this work were carried out as part of the Green Infrastructure and the Health and Well-Being Influences on an Ageing Population (GHIA) project (2016–2019) http://www.ghia.org.uk. This project is funded by the Natural Environment Research Council, the Arts and Humanities Research Council and the Economic and Social Research Council under the Valuing Nature Programme. NERC grant reference number NE/N013530/1.

Appendix A. Supplementary data

Supplementary data to this article can be found online at https://doi.org/10.1016/j.scitotenv.2020.143050.

References

Acharya, A.S., Prakash, A., Saxena, P., Nigam, A., 2013. Sampling: why and how of it. Indian Journal of Medical Specialties 4 (2), 330–333. https://doi.org/10.7713/ijms.2013.0032.

Anderson, Carl C., Rex, Art, 2019. Preserving the scenic views from North Carolina's Blue Ridge Parkway: A decision support system for strategic land conservation planning. Appl. Geogr. 104, 75–82. https://doi.org/10.1016/j.apgeog.2019.01.008.

Anguelov, D., Dulong, C., Filip, D., Frueh, C., Lafon, S., Lyon, R., Ogale, A., Vincent, L., Weaver, J., 2010. Google street view: capturing the world at street level. Computer 43 (6), 32–38. https://doi.org/10.1109/MC.2010.170.

Bell, S., 2012. Landscape: Pattern, Perception and Process. Routledge.

Bishop, I.D., 2002. Determination of thresholds of visual impact: the case of wind turbines. Environment and Planning B: Planning and design 29 (5), 707–718. https://doi.org/10.1068/b12854.

Bratman, G.N., Anderson, C.B., Berman, M.G., Cochran, B., De Vries, S., Flanders, J., Folke, C., Frumkin, H., Gross, J.J., Hartig, T., Kahn, P.H., 2019. Nature and mental health: an ecosystem service perspective. Sci. Adv. 5 (7), eaax0903. https://doi.org/10.1126/sciadv.aax0903.

Bresenham, J.E., 1965. Algorithm for computer control of a digital plotter. IBM Syst. J. 4 (1), 25–30.

Bresenham, J., 1977. A linear algorithm for incremental digital display of circular arcs. Commun. ACM 20 (2), 100–106.

Brindley, P., Jorgensen, A., Maheswaran, R., 2018. Domestic gardens and self-reported health: a national population study. Int. J. Health Geogr. 17 (1), 31. https://doi.org/10.1186/s12942-018-0148-6.

Brown, D.K., Barton, J.L., Gladwell, V.F., 2013. Viewing nature scenes positively affects recovery of autonomic function following acute-mental stress. Environmental science & technology 47 (11), 5562–5569. https://doi.org/10.1021/es305019p.

Browning, M., Lee, K., 2017. Within what distance does "greenness" best predict physical health? A systematic review of articles with GIS buffer analyses across the lifespan. Int. J. Environ. Res. Public Health 14 (7), 675. https://doi.org/10.3390/ijerph14070675.

Browning, M.H., Mimnaugh, K.J., van Riper, C.J., Laurent, H.K., LaValle, S.M., 2019. Can simulated nature support mental health? Comparing short, single-doses of 360-degree nature videos in virtual reality with the outdoors. Front. Psychol., 10 https://doi.org/10.3389/fpsyg.2019.02667.

Brughmans, T., van Garderen, M., Gillings, M., 2018. Introducing visual neighbourhood configurations for total viewsheds. J. Archaeol. Sci. 96, 14–25. https://doi.org/10.1016/j.jas.2018.05.006.

Cao, M., Liu, S., Cao, F., 2020, January. Midpoint distance circle generation algorithm based on midpoint circle algorithm and Bresenham circle algorithm. In. J. Phys. Conf. Ser. 1438 (1), 012017 IOP Publishing. https://doi.org/10.1088/1742-6596/1438/1/012017.

Carver, S., Washtell, J., 2012, April. Real-time visibility analysis and rapid viewshed calculation using a voxel-based modelling approach. GISRUK 2012 conference. vol. 11 apr.

Chamberlain, B.C., Meitner, M.J., 2013. A route-based visibility analysis for landscape management. Landsc. Urban Plan. 111, 13–24. https://doi.org/10.1016/j.landurbplan.2012.12.004.

Chen, X., Meng, Q., Hu, D., Zhang, L., Yang, J., 2019. Evaluating greenery around streets using Baidu panoramic street view images and the panoramic green view index. Forests 10 (12), 1109. https://doi.org/10.3390/f10121109.

Chen, Ziyue, Xu, Bing, Gao, Bingbo, 2015. Assessing visual green effects of individual urban trees using airborne Lidar data. Sci. Total Environ. 536, 232–244. https://doi.org/10.1016/j.scitotenv.2015.06.142.

Chen, J., Zhou, C., Li, F., 2020. Quantifying the green view indicator for assessing urban greening quality: an analysis based on internet-crawling street view data. Ecol. Indic. 113, 106192. https://doi.org/10.1016/j.ecolind.2020.106192.

Chung, K.L., Huang, Y.H., 2007. Speed up the computation of randomised algorithms for detecting lines, circles, and ellipses using novel tuning-and LUT-based voting platform. Appl. Math. Comput. 190 (1), 132–149. https://doi.org/10.1016/j.amc.2007.01.012.

Church, S.P., 2018. From street trees to natural areas: retrofitting cities for human connectedness to nature. J. Environ. Plan. Manag. 61 (5–6), 878–903. https://doi.org/10.1080/09640568.2018.1428182.

City of Trees, 2011. Cityoftrees.org.uk; Greater Manchester Tree Audit [computer File]. Personal communication, Manchester, UK.

Clayton, S., 2007. Domesticated nature: motivations for gardening and perceptions of environmental impact. J. Environ. Psychol. 27 (3), 215–224. https://doi.org/10.1016/j.jenvp.2007.06.001.

Dadvand, P., Nieuwenhuijsen, M., 2019. Green space and health. Integrating Human Health into Urban and Transport Planning. Springer, Cham, pp. 409–423 https://doi.org/10.1007/978-3-319-74983-9_20.

Daniela, D.A., Gola, M., Letizia, A., Marco, D., Fara, G.M., Rebecchi, A., Gaetano, S., Capolongo, S., 2020. COVID-19 and living spaces challenge. Well-being and public health recommendations for a healthy, safe, and sustainable housing. Acta Biomed 91, 9–S. https://doi.org/10.23750/abm.v91i9-S.10115.

de Bell, S., White, M., Griffiths, A., Darlow, A., Taylor, T., Wheeler, B., Lovell, R., 2020. Spending time in the garden is positively associated with health and wellbeing: results from a national survey in England. Landsc. Urban Plan. 200, 103836. https://doi.org/10.1016/j.landurbplan.2020.103836.

Defra Data Services Platform, 2020. LIDAR Composite DSM 2017 - 2m. [online] Available at. https://environment.data.gov.uk/dataset/e9edb9f6-d563-4a5e-a425-c72c5eac919c. (Accessed 14 June 2020).

Dennis, M., Barlow, D., Cavan, G., Cook, P.A., Gilchrist, A., Handley, J., James, P., Thompson, J., Tzoulas, K., Wheater, C.P., Lindley, S., 2018. Mapping urban green infrastructure: a novel landscape-based approach to incorporating land use and land cover in the mapping of human-dominated systems. Land 7 (1), 17. https://doi.org/10.3390/land7010017.

Dennis, M., Cook, P.A., James, P., Wheater, C.P., Lindley, S.J., 2020. Relationships between health outcomes in older populations and urban green infrastructure size, quality and proximity. BMC Public Health 20, 1–15. https://doi.org/10.1186/s12889-020-08762-x.

Díaz, S., Pascual, U., Stenseke, M., Martín-López, B., Watson, R.T., Molnár, Z., Hill, R., Chan, K.M.A., Baste, I.A., Brauman, K.A., et al., 2018. Assessing nature's contributions to people. Science 359, 270–272. https://doi.org/10.1126/science.aap8826.

Domingo-Santos, J.M., de Villarán, R.F., Rapp-Arrarás, Í., de Provens, E.C.P., 2011. The visual exposure in forest and rural landscapes: an algorithm and a GIS tool. Landsc. Urban Plan. 101 (1), 52–58. https://doi.org/10.1016/j.landurbplan.2010.11.018.

Environment Agency, 2019a. Lidar composite digital surface model England 2m resolution [ASC geospatial data], scale 1:8000, tile: SJ89. Updated: 5 January 2016, Open Government Licence, Using: EDINA LIDAR Digimap Service. https://digimap.edina.ac.uk.

Environment Agency (2019b). Lidar composite digital terrain model England 2m resolution [ASC geospatial data], scale 1:8000, tile: SJ89, Updated: 5 January 2016, Open Government Licence, Using: EDINA LIDAR Digimap Service, https://digimap.edina.ac.uk, Downloaded: 2019-03-28.

Feng, W., Gang, W., Deji, P., Yuan, L., Liuzhong, Y., Hongbo, W., 2015. A parallel algorithm for viewshed analysis in three-dimensional digital earth. Comput. Geosci. 75, 57–65. https://doi.org/10.1016/j.cageo.2014.10.012.

Fisher, P.F., 1996. Extending the applicability of viewsheds in landscape planning. Photogramm. Eng. Remote. Sens. 62 (11), 1297–1302.

Freeman, C., Dickinson, K.J., Porter, S., van Heezik, Y., 2012. "My garden is an expression of me": exploring householders' relationships with their gardens. J. Environ. Psychol. 32 (2), 135–143. https://doi.org/10.1016/j.jenvp.2012.01.005.

Frumkin, H., Bratman, G.N., Breslow, S.J., Cochran, B., Kahn Jr., P.H., Lawler, J.J., Levin, P.S., Tandon, P.S., Varanasi, U., Wolf, K.L., Wood, S.A., 2017. Nature contact and human health: a research agenda. Environ. Health Perspect. 125 (7), 075001. https://doi.org/10.1289/EHP1663.

Fry, D., Mooney, S.J., Rodríguez, D.A., Caiaffa, W.T., Lovasi, G.S., 2020. Assessing Google street view image availability in Latin American cities. J. Urban Health, 1–9 https://doi.org/10.1007/s11524-019-00408-7.

Furnari, A., Farinella, G.M., Bruna, A.R., Battiato, S., 2016. Affine covariant features for fisheye distortion local modeling. IEEE Trans. Image Process. 26 (2), 696–710. https://doi.org/10.1109/TIP.2016.2627816.

GMCA, 2019. Greater Manchester's plan for homes, jobs and the environment- GREATER MANCHESTER SPATIAL FRAMEWORK. Available at. https://www.greatermanchester-ca.gov.uk/media/1710/gm_plan_for_homes_jobs_and_the_environment_1101-web.pdf. (Accessed 20 January 2020).

Hazer, M., Formica, M.K., Dieterlen, S., Morley, C.P., 2018. The relationship between self-reported exposure to greenspace and human stress in Baltimore, MD. Landsc. Urban Plan. 169, 47–56. https://doi.org/10.1016/j.landurbplan.2017.08.006.
Helbich, M., 2018. Toward dynamic urban environmental exposure assessments in mental health research. Environ. Res. 161, 129–135. https://doi.org/10.1016/j.envres.2017.11.006.
Helbich, M., Yao, Y., Liu, Y., Zhang, J., Liu, P., Wang, R., 2019. Using deep learning to examine street view green and blue spaces and their associations with geriatric depression in Beijing, China. Environ. Int. 126, 107–117. https://doi.org/10.1016/j.envint.2019.02.013.
Huang, W.Z., Yang, B.Y., Yu, H.Y., Bloom, M.S., Markevych, I., Heinrich, J., Knibbs, L.D., Leskinen, A., Dharmage, S.C., Jalaludin, B., Morawska, L., 2020. Association between community greenness and obesity in urban-dwelling Chinese adults. Sci. Total Environ. 702, 135040. https://doi.org/10.1016/j.scitotenv.2019.135040.
Hughes, C., Glavin, M., Jones, E., Denny, P., 2008. Review of geometric distortion compensation in fish-eye cameras. IET Irish Signals and Systems Conference (ISSC 2008). IET, pp. 162–167 https://doi.org/10.1049/cp:20080656.
James, P., Banay, R.F., Hart, J.E., Laden, F., 2015. A review of the health benefits of greenness. Current Epidemiology Reports 2 (2), 131–142. https://doi.org/10.1007/s40471-015-0043-7.
Jiang, B., Deal, B., Pan, H., Larsen, L., Hsieh, C.H., Chang, C.Y., Sullivan, W.C., 2017. Remotely-sensed imagery vs. eye-level photography: evaluating associations among measurements of tree cover density. Landsc. Urban Plan. 157, 270–281. https://doi.org/10.1016/j.landurbplan.2016.07.010.
Kaplan, S., 1995. The restorative benefits of nature: toward an integrative framework. J. Environ. Psychol. 15 (3), 169–182. https://doi.org/10.1016/0272-4944(95)90001-2.
Kaplan, R., 2001. The nature of the view from home: psychological benefits. Environ. Behav. 33 (4), 507–542. https://doi.org/10.1177/00139160121973115.
Kaplan, R., Kaplan, S., 1989. The Experience of Nature: A Psychological Perspective. CUP Archive.
Kappel, M.R., 1985. An ellipse-drawing algorithm for raster displays. Fundamental Algorithms for Computer Graphics. Springer, Berlin, Heidelberg, pp. 257–280 https://doi.org/10.1007/978-3-642-84574-1_13.
Kumakoshi, Y., Chan, S.Y., Koizumi, H., Li, X., Yoshimura, Y., 2020. Standardized green view index and quantification of different metrics of urban green vegetation. Sustainability 12 (18), 7434. https://doi.org/10.3390/su12187434.
Kumsap, C., Borne, F., Moss, D., 2005. The technique of distance decayed visibility for forest landscape visualisation. Int. J. Geogr. Inf. Sci. 19 (6), 723–744. https://doi.org/10.1080/13658810500104880.
Kuo, M., Browning, M.H., Sachdeva, S., Lee, K., Westphal, L., 2018. Might school performance grow on trees? Examining the link between "greenness" and academic achievement in urban, high-poverty schools. Front. Psychol. 9, 1669. https://doi.org/10.3389/fpsyg.2018.01669.
Labib, S.M., 2019. Investigation of the likelihood of green infrastructure (GI) enhancement along linear waterways or on derelict sites (DS) using machine learning. Environ. Model Softw. 118, 146–165. https://doi.org/10.1016/j.envsoft.2019.05.006.
Labib, S.M., Harris, A., 2018. The potentials of Sentinel-2 and LandSat-8 data in green infrastructure extraction, using object based image analysis (OBIA) method. European Journal of Remote Sensing 51 (1), 231–240. https://doi.org/10.1080/22797254.2017.1419441.
Labib, S.M., Lindley, S., Huck, J.J., 2020a. Spatial dimensions of the influence of urban green-blue spaces on human health: a systematic review. Environ. Res. 180, 108869. https://doi.org/10.1016/j.envres.2019.108869.
Labib, S.M., Lindley, S., Huck, J.J., 2020b. Scale effects in remotely sensed greenspace metrics and how to mitigate them for environmental health exposure assessment. Comput. Environ. Urban. Syst. 82, 101501. https://doi.org/10.1016/j.compenvurbsys.2020.101501.
Larkin, A., Hystad, P., 2019. Evaluating street view exposure measures of visible green space for health research. Journal of Exposure Science & Environmental Epidemiology 29 (4), 447–456. https://doi.org/10.1038/s41370-018-0017-1.
Lecun, Y., Bengio, Y., Hinton, G., 2015. Deep learning. Nature https://doi.org/10.1038/nature14539.
Li, X., Ghosh, D., 2018. Associations between body mass index and urban "green" streetscape in Cleveland, Ohio, USA. Int. J. Environ. Res. Public Health 15 (10), 2186. https://doi.org/10.3390/ijerph15102186.
Li, X., Zhang, C., Li, W., Ricard, R., Meng, Q., Zhang, W., 2015. Assessing street-level urban greenery using Google street view and a modified green view index. Urban For. Urban Green. 14 (3), 675–685. https://doi.org/10.1016/j.ufug.2015.06.006.
Lindley, S.J., Cook, P.A., Dennis, M., Gilchrist, A., 2019. Biodiversity, physical health and climate change: a synthesis of recent evidence. Biodiversity and Health in the Face of Climate Change. Springer, Cham, pp. 17–46 https://doi.org/10.1007/978-3-030-02318-8_2.
Liu, Y., Wang, R., Lu, Y., Li, Z., Chen, H., Cao, M., Zhang, Y., Song, Y., 2020. Natural outdoor environment, neighbourhood social cohesion and mental health: using multi-level structural equation modelling, streetscape and remote-sensing metrics. Urban For. Urban Green. 48, 126576. https://doi.org/10.1016/j.ufug.2019.126576.
Lottrup, L., Grahn, P., Stigsdotter, U.K., 2013. Workplace greenery and perceived level of stress: benefits of access to a green outdoor environment at the workplace. Landsc. Urban Plan. 110, 5–11. https://doi.org/10.1016/j.landurbplan.2012.09.002.
Lu, Y., 2019. Using Google street view to investigate the association between street greenery and physical activity. Landsc. Urban Plan. 191, 103435. https://doi.org/10.1016/j.landurbplan.2018.08.029.
Lu, Y., Sarkar, C., Xiao, Y., 2018. The effect of street-level greenery on walking behavior: evidence from Hong Kong. Soc. Sci. Med. 208, 41–49. https://doi.org/10.1016/j.socscimed.2018.05.022.
Lu, Y., Yang, Y., Sun, G., Gou, Z., 2019. Associations between overhead-view and eye-level urban greenness and cycling behaviors. Cities 88, 10–18. https://doi.org/10.1016/j.cities.2019.01.003.
Markevych, I., Schoierer, J., Hartig, T., Chudnovsky, A., Hystad, P., Dzhambov, A.M., De Vries, S., Triguero-Mas, M., Brauer, M., Nieuwenhuijsen, M.J., Lupp, G., 2017. Exploring pathways linking greenspace to health: theoretical and methodological guidance. Environ. Res. 158, 301–317. https://doi.org/10.1016/j.envres.2017.06.028.
Marsh, E.J., Schreiber, K., 2015. Eyes of the empire: a viewshed-based exploration of Wari site-placement decisions in the Sondondo Valley, Peru. J. Archaeol. Sci. Rep. 4, 54–64. https://doi.org/10.1016/j.jasrep.2015.08.031.
Martínez-Graña, A.M., Silva, P.G., Goy, J.L., Elez, J., Valdés, V., Zazo, C., 2017. Geomorphology applied to landscape analysis for planning and management of natural spaces. Case study: Las Batuecas-S. de Francia and Quilamas natural parks (Salamanca, Spain). Sci. Total Environ. 584, 175–188. https://doi.org/10.1016/j.scitotenv.2017.01.155.
Mavoa, S., Davern, M., Breed, M., Hahs, A., 2019. Higher levels of greenness and biodiversity associate with greater subjective wellbeing in adults living in Melbourne, Australia. Health & Place 57, 321–329. https://doi.org/10.1016/j.healthplace.2019.05.006.
McDougall, C.W., Quilliam, R.S., Hanley, N., Oliver, D.M., 2020. Freshwater blue space and population health: an emerging research agenda. Sci. Total Environ. 737, 140196. https://doi.org/10.1016/j.scitotenv.2020.140196.
Mitchell, R. and Popham, F., 2008. Effect of exposure to natural environment on health inequalities: an observational population study. Lancet, 372(9650), pp.1655–1660. DOI: https://doi.org/10.1016/S0140-6736(08)61689-X.
Nutsford, D., Reitsma, F., Pearson, A.L., Kingham, S., 2015. Personalising the viewshed: visibility analysis from the human perspective. Appl. Geogr. 62, 1–7. https://doi.org/10.1016/j.apgeog.2015.04.004.
Nutsford, D., Pearson, A.L., Kingham, S., Reitsma, F., 2016. Residential exposure to visible blue space (but not green space) associated with lower psychological distress in a capital city. Health & place 39, 70–78. https://doi.org/10.1016/j.healthplace.2016.03.002.
Office for National Statistics, 2011. Office for National Statistics 2011 Census - Office for National Statistics(2012) [online]. Available at:. https://www.ons.gov.uk/peoplepopulationandcommunity/populationandmigration/populationestimates/bulletins/2011censuspopulationandhouseholdestimatesforsmallareasinenglandandwales/2012-11-23. (Accessed 15 July 2020).
Openshaw, S., 1981. The modifiable areal unit problem. Quantitative Geography: A British View 60–69.
OS MasterMap, 2019. Building Heights [FileGeoDatabase geospatial data], Scale 1:2500, Updated: 23 October 2017, Ordnance Survey (GB), Using: EDINA Digimap Ordnance Survey Service. Available at:. https://digimap.edina.ac.uk.
Palmer, J.F., 2019. The contribution of a GIS-based landscape assessment model to a scientifically rigorous approach to visual impact assessment. Landsc. Urban Plan. 189, 80–90. https://doi.org/10.1016/j.landurbplan.2019.03.005.
Qiang, Y., Shen, S., Chen, Q., 2019. Visibility analysis of oceanic blue space using digital elevation models. Landsc. Urban Plan. 181, 92–102. https://doi.org/10.1016/j.landurbplan.2018.09.019.
Russell, R., Guerry, A.D., Balvanera, P., Gould, R.K., Basurto, X., Chan, K.M., Klain, S., Levine, J., Tam, J., 2013. Humans and nature: how knowing and experiencing nature affect wellbeing. Annu. Rev. Environ. Resour. 38, 473–502. https://doi.org/10.1146/annurev-environ-012312-110838.
Rzotkiewicz, A., Pearson, A.L., Dougherty, B.V., Shortridge, A., Wilson, N., 2018. Systematic review of the use of Google street view in health research: major themes, strengths, weaknesses and possibilities for future research. Health & place 52, 240–246. https://doi.org/10.1016/j.healthplace.2018.07.001.
Sahraoui, Y., Clauzel, C., Foltête, J.C., 2016. Spatial modelling of landscape aesthetic potential in urban-rural fringes. J. Environ. Manag. 181, 623–636. https://doi.org/10.1016/j.jenvman.2016.06.031.
Silva, R.A., Rogers, K., Buckley, T.J., 2018. Advancing environmental epidemiology to assess the beneficial influence of the natural environment on human health and well-being. Environmental science & technology 52 (17), 9545–9555. https://doi.org/10.1021/acs.est.8b01781.
Stubbings, P., Peskett, J., Rowe, F., Arribas-Bel, D., 2019. A hierarchical urban forest index using street-level imagery and deep learning. Remote Sens. 11 (12), 1395. https://doi.org/10.3390/rs11121395.
Tabrizian, P., Baran, P.K., Van Berkel, D., Mitasova, H., Meentemeyer, R., 2020. Modeling restorative potential of urban environments by coupling viewscape analysis of lidar data with experiments in immersive virtual environments. Landsc. Urban Plan. 195, 103704. https://doi.org/10.1016/j.landurbplan.2019.103704.
Taylor, P.J., Openshaw, S., 1975. Distance decay in spatial interactions. Concepts and Techniques in Modern Geography.
Tzoulas, K., Korpela, K., Venn, S., Yli-Pelkonen, V., Kaźmierczak, A., Niemela, J., James, P., 2007. Promoting ecosystem and human health in urban areas using green infrastructure: a literature review. Landsc. Urban Plan. 81 (3), 167–178. https://doi.org/10.1016/j.landurbplan.2007.02.001.
Ulrich, R., 1984. View through a window may influence recovery. Science 224 (4647), 224–225. https://doi.org/10.1126/science.6143402.
Ulrich, R.S., Simons, R.F., Losito, B.D., Fiorito, E., Miles, M.A. and Zelson, M., 1991. Stress recovery during exposure to natural and urban environments. J. Environ. Psychol., 11 (3), pp.201–230. DOI: https://doi.org/10.1016/S0272-4944(05)80184-7.
Van Aken, J.R., 1984. An efficient ellipse-drawing algorithm. IEEE Comput. Graph. Appl. 4 (9), 24–35. https://doi.org/10.1109/MCG.1984.275994.
Van Berkel, D.B., Tabrizian, P., Dorning, M.A., Smart, L., Newcomb, D., Mehaffey, M., Neale, A., Meentemeyer, R.K., 2018. Quantifying the visual-sensory landscape qualities that

contribute to cultural ecosystem services using social media and LiDAR. Ecosystem services 31, 326–335. https://doi.org/10.1016/j.ecoser.2018.03.022.

Van Herzele, A., de Vries, S., 2012. Linking green space to health: a comparative study of two urban neighbourhoods in Ghent, Belgium. Popul. Environ. 34 (2), 171–193. https://doi.org/10.1007/s11111-011-0153-1.

Wang, R., Helbich, M., Yao, Y., Zhang, J., Liu, P., Yuan, Y., Liu, Y., 2019. Urban greenery and mental wellbeing in adults: cross-sectional mediation analyses on multiple pathways across different greenery measures. Environ. Res. 176, 108535. https://doi.org/10.1016/j.envres.2019.108535.

Wang, R., Yang, B., Yao, Y., Bloom, M.S., Feng, Z., Yuan, Y., Zhang, J., Liu, P., Wu, W., Lu, Y., Baranyi, G., 2020. Residential greenness, air pollution and psychological wellbeing among urban residents in Guangzhou, China. Sci. Total Environ. 711, 134843. https://doi.org/10.1016/j.scitotenv.2019.134843.

Yang, J., Zhao, L., Mcbride, J., Gong, P., 2009. Can you see green? Assessing the visibility of urban forests in cities. Landsc. Urban Plan. 91 (2), 97–104. https://doi.org/10.1016/j.landurbplan.2008.12.004.

Yang, Y., He, D., Gou, Z., Wang, R., Liu, Y., Lu, Y., 2019. Association between street greenery and walking behavior in older adults in Hong Kong. Sustain. Cities Soc. 51, 101747. https://doi.org/10.1016/j.scs.2019.101747.

Ye, Y., Richards, D., Lu, Y., Song, X., Zhuang, Y., Zeng, W., Zhong, T., 2019. Measuring daily accessed street greenery: a human-scale approach for informing better urban planning practices. Landsc. Urban Plan. 191, 103434. https://doi.org/10.1016/j.landurbplan.2018.08.028.

Yu, S., Yu, B., Song, W., Wu, B., Zhou, J., Huang, Y., Wu, J., Zhao, F., Mao, W., 2016. View-based greenery: a three-dimensional assessment of city buildings' green visibility using floor green view index. Landsc. Urban Plan. 152, 13–26. https://doi.org/10.1016/j.landurbplan.2016.04.004.

Yu, X., Zhao, G., Chang, C., Yuan, X., Heng, F., 2019. Bgvi: a new index to estimate street-side greenery using baidu street view image. Forests 10 (1), 3. https://doi.org/10.3390/f10010003.

Zhan, Y., Liu, J., Lu, Z., Yue, H., Zhang, J., Jiang, Y., 2020. Influence of residential greenness on adverse pregnancy outcomes: a systematic review and dose-response meta-analysis. Sci. Total Environ. 718, 137420. https://doi.org/10.1016/j.scitotenv.2020.137420.

Zhou, B., Zhao, H., Puig, X., Xiao, T., Fidler, S., Barriuso, A., Torralba, A., 2019. Semantic understanding of scenes through the ade20k dataset. Int. J. Comput. Vis. 127 (3), 302–321. https://doi.org/10.1007/s11263-018-1140-0.